Atmos. Chem. Phys. Discuss., 2, 289–337, 2002
www.atmos-chem-phys.org/acpd/2/289/

Atmospheric Chemistry and Physics Discussions

Greenhouse effect dependence on atmospheric concentrations of greenhouse substances and the nature of climate stability on Earth

V. G. Gorshkov and A. M. Makarieva

Petersburg Nuclear Physics Institute, 188300, Gatchina, St.-Petersburg, Russia

Received: 22 January 2002 – Accepted: 16 February 2002 – Published: 8 March 2002

Correspondence to: A. M. Makarieva (elba@infopro.spb.su)

Abstract

Due to the exponential positive feedback between sea surface temperature and saturated water vapour concentration, dependence of the planetary greenhouse effect on atmospheric water content is critical for stability of a climate with extensive liquid hydrosphere.

In this paper on the basis of the law of energy conservation we develop a simple physically transparent approach to description of radiative transfer in an atmosphere containing greenhouse substances. It is shown that the analytical solution of the equation thus derived coincides with the exact solution of the well-known radiative transfer equation to the accuracy of 20% for all values of atmospheric optical depth. The derived equation makes it possible to easily take into account the non-radiative thermal fluxes (convection and latent heat) and obtain an analytical dependence of the greenhouse effect on atmospheric concentrations of a set of greenhouse substances with arbitrary absorption intervals.

The established dependence is used to analyse stability of the modern climate of Earth. It is shown that the modern value of global mean surface temperature, which corresponds to the liquid state of the terrestrial hydrosphere, is physically unstable. The observed stability of modern climate over geological timescales is therefore likely to be due to dynamic singularities in the physical temperature-dependent behaviour of the greenhouse effect. We hypothesise that such singularities may appear due to controlling functioning of the natural global biota and discuss major arguments in support of this conclusion.

1 Introduction

Climate stability is determined by the values and temperature-dependent behaviour of the planetary albedo and atmospheric greenhouse effect. At zero albedo and in the absence of the greenhouse effect, temperature of the planet's surface is dictated by

the incoming flux of solar energy, i.e. by the orbital position the planet occupies in the solar system. Below this temperature is called orbital. Values of albedo common to planets of the solar system correspond to decrease of the surface temperature by no more than several tens of degrees Kelvin. By contrast, the greenhouse effect may increase surface temperature by several hundred degrees Kelvin, as it takes place on Venus (Mitchell, 1989).

The Earth's orbital temperature is equal to +5°C. The Earth's albedo, which is likely to approach its minimum possible value for ordinary planetary surfaces, would, in the absence of a greenhouse effect, lower the surface temperature down to −18°C. The modern greenhouse effect increases the global mean surface temperature of the planet by 33°C, up to +15°C.

The overwhelming part of the greenhouse effect on Earth is determined by atmospheric water vapour, cloudiness and CO_2. Due to the presence of large amounts of liquid water on the planet's surface, the atmospheric water content grows exponentially with increasing surface temperature. This positive feedback can in principle lead to an unlimited increase of the greenhouse effect and surface temperature, until the oceans evaporate completely. The possibility of such a "runaway" greenhouse effect has been repeatedly discussed in the literature (Ingersoll, 1976; Rasool and de Berg, 1979; Nakajima et al., 1992; Weaver and Ramanathan, 1995).

Changing the values of albedo and greenhouse effect, it is possible to equate the incoming flux of short-wave solar radiation absorbed by the planet and the outgoing flux of long-wave radiation emitted by the planet into space. This equality determines a stationary equilibrium temperature of the Earth's surface. However, due to the positive feedback outlined above, such an equilibrium may appear to be unstable. Any small fluctuations will be then able to drive the surface temperature either in the direction of cooling, towards the planet's glaciation, or in the direction of warming, towards complete evaporation of the hydrosphere.

In the studies of the runaway greenhouse effect (Ingersoll, 1976; Rasool and de Berg, 1979; Nakajima et al., 1992; Weaver and Ramanathan, 1995) one addresses

the problem of whether the existence of an equilibrium surface temperature at different values of solar constant is possible or not. Stability of the equilibrium temperature, should such an equilibrium exist, is rarely discussed. The possibility of an equilibrium global mean surface temperature being unstable was mentioned by Ingersoll (1967).

Modern climate of Earth is stable, as testified for by the observations that oscillations of the global mean surface temperature did not exceed 10°C during the last several hundred million years (Berggren and Van Couvering, 1986), several degrees Celsius – during the last ten thousand years, and several fractions of degree Celsius – during the last century (Savin, 1977; Watts, 1982). It follows that in the vicinity of the modern value of the global mean surface temperature there are certain negative feedbacks in action, that overcome the positive greenhouse feedback discussed above.

These negative feedbacks are manifested as empirically established regularities in the temperature-dependent behaviour of various climate-forming factors. Climate models that incorporate these regularities yield, as expected, a stable equilibrium surface temperature (Manabe and Wetherald, 1967; North and Coakley, 1979; North et al., 1981; Dickinson, 1985). In the meantime, there are no theoretical studies that would predict or explain the observed stability of the modern Earth's climate *a priori*, on the basis of the known physical laws.

This paper aims at establishing a theoretical dependence of the greenhouse effect on atmospheric concentrations of greenhouse substances, which is then used in the analysis of the nature of stability of the modern Earth's climate. In Sects. 2 and 3 we show that the equation of transfer of thermal radiation in a given spectral interval can be reasonably approximated by an equation of the diffusion (heat conductivity) type for all values of atmospheric optical depth τ. In the case of radiative equilibrium, solution of the corresponding diffusion equation represents a linear dependence of the upward flux of long-wave radiation at the surface on the atmospheric optical thickness τ_s, which differs from the exact solution of the radiative transfer equation by no more than 20% for all values of τ_s.

In Sect. 4 we employ standard methods for accounting in the diffusion equation for

non-radiative thermal fluxes of convection and latent heat. It is shown that such an account retains the linear dependence of the upward flux of thermal radiation at the surface on the atmospheric optical thickness τ_s in a definite spectral interval. It is only the slope of the corresponding line that is changed. In Sect. 5 we derive an analytical formula for the dependence of the greenhouse effect (defined here as the difference between thermal fluxes at the surface and outside the atmosphere) on atmospheric concentrations of greenhouse substances and use it in the theoretical analysis of stability of possible Earth's climates. It is shown that a climate with a liquid hydrosphere is physically unstable. In Sect. 6 the available empirical data are employed to quantify deviations of the real greenhouse effect from the theoretical physical behaviour, that are necessary to explain the observed stability of modern climate of Earth. In Sect. 7 (Conclusions) we analyse possible reasons for the observed climate stability and hypothesize that it is due to the controlling functioning of the global natural biota, discussing major arguments in support of this hypothesis.

2 Propagation of thermal photons in a stratified atmosphere

After averaging over latitude and longitude, as well as over diurnal and seasonal oscillations, all measurable characteristics of the atmosphere may only depend on height z. Such averaging corresponds to the planar (stratified) atmosphere (Chandrasekhar, 1950; Michalas and Michalas, 1984), which differs from the one-dimensional atmosphere, where all radiation propagates along z-axis only, by allowing the beams to form an arbitrary angle with the vertical axis.

Photons emitted from the Earth's surface travel on average a distance equal to the mean free path l, before they are absorbed by molecules of greenhouse substances and further re-emitted with an equal probability (in the case of isotropy) in either upward or downward direction. A photon emitted downwards is absorbed by the Earth's surface and re-emitted upwards. A photon emitted upwards travels on average another free path l, after which it is absorbed by the next molecule, and so forth. Averaging

over a large number of thermal photons, we obtain pattern shown in Fig. 1. In Fig. 1 the atmosphere is divided into m layers, the distance between any two neighbouring layers being equal to the mean free path of thermal photons. Each layer absorbs thermal photons coming from the two neighbouring layers (the lower and the upper) only. The absorbed photons are emitted up and down with an equal probability. Variable m corresponds to optical thickness of the atmosphere.

The proposed consideration, Fig. 1, would be exact, if the standard deviation of the free path length l – distance covered by photons without interaction with greenhouse molecules – were negligibly small compared to the mean free path length. In the real case of space uniformity, the probability of absorption is the same along all the path traveled by the photon. Thus, the probability of covering a path z without collisions becomes $\exp(-z/l)$. Accordingly, the standard deviation of free path length coincides with the mean free path length l. In terms of Fig. 1, it means that each of the m layers, that are infinitely thin in Fig. 1, spreads approximately to the point where it meets with the neighbouring one. Yet such expanded layers do not overlap significantly. Thus, the possible inaccuracy of our consideration, caused by neglecting the absorption events that take place at a distance further than one standard deviation, is unlikely to change the order of magnitude of the results to be obtained.

The inaccuracy of the representation in Fig. 1 would decrease, if one "pushed" the layers apart at a distance exceeding the mean free path length l. Then a larger fraction of absorption events can be formally taken into account as taking place between any two neighbouring layers. However, in such a case a considerable portion of photons emitted by a given layer would not reach the neighbouring layers. As a result, the condition of energy conservation for radiative interaction between the neighbouring layers in Fig. 1, will not be applicable. Thus, l remains as the only scale factor of the considered problem. It can be expected therefore that a satisfactory solution with a minimum inaccuracy can be obtained by multiplication of l by a geometric factor between 1 and 2. By analysing the exact radiation transfer equation in Section 2 we will show that this factor is about 1.2 for the three-dimensional planar atmosphere. Once

this factor is taken into account, the inaccuracy of the simple consideration offered in this section does not exceed 15% for any value of m.

Let F_k be the upward flux of thermal radiation from the k-th layer, dimension [W m^{-2}], equal to the downward flux from the same layer. Then $F_s \equiv F_{m+1}$ is the upward flux of thermal radiation from the Earth's surface, $F_1 = F_e$ is the upward flux of thermal radiation outside the atmosphere. In the case of radiative equilibrium, we obtain the following system of recurrent equations (see Fig. 1):

$$\begin{aligned} &F_1 = F_e, \quad 2F_1 = F_2, \quad \ldots \quad 2F_k = F_{k+1} + F_{k-1} \quad \ldots \\ &F_s \equiv F_{m+1} = F_m + F_e, \quad 2 \le k \le m, \end{aligned} \tag{2.1}$$

where k increases in the downward direction. The first equation in (2.1) expresses the boundary condition at the top of the atmosphere, while the remaining equations are based on the law of energy conservation at each layer, including the Earth's surface. Solution of Eq. (2.1) for any $1 \le k \le m + 1$ is:

$$F_k = kF_e, \quad F_s \equiv F_{m+1} = (1 + m)F_e\,. \tag{2.2}$$

Equations (2.1) and their solution (2.2) are valid for one greenhouse substance absorbing radiation in a finite spectral interval, as well as for a "grey" medium with absorption interval expanding over the whole thermal spectrum. When there are N different types of greenhouse substances with absorption intervals in different parts of the thermal spectrum, solution (2.2) remains valid for every particular absorption interval in the realistic case of resonance scattering (absorption and emision of thermal radiation). Taking into account that the thermal radiative flux of the Earth's surface is close to blackbody radiative flux described by Planck's formula, $I_P(\lambda, T)$, one can represent the surface radiation in a given spectral interval $\Delta\lambda_i = \lambda_2 - \lambda_1$ as $F_s\delta_i$, where

$$\delta_i = \frac{\int_{\lambda_1}^{\lambda_2} I_P(\lambda, T)\,d\lambda}{\sigma_R T^4}, \quad F_s = \sigma_R T^4, \quad \sum_{i=1}^{N} \delta_i = 1\,. \tag{2.3}$$

Here σ_R is the Stephen-Boltzmann constant. In this paper we do not use either local air temperature or the assumption of local thermodynamic equilibrium in the atmosphere. Using Eq. (2.3), one may write Eq. (2.2) as

$$\begin{aligned} &F_s\delta_i = (1 + m_i + m_0)\,F_{ei}, \quad m_i = \frac{h_i}{l_i} = h_i\,\sigma_i\,n_i \\ &\sum_{i=1}^{N} F_{ei} = F_e, \quad b \equiv \frac{F_e}{F_s} = \sum_{i=1}^{N} \frac{\delta_i}{1 + m_i + m_0} \end{aligned} \tag{2.4}$$

Here $m_0 = h_0/l_0 = h_0\sigma_0 n_0$ is the optical thickness of cloudiness, which absorbs radiation rather evenly over the whole thermal spectrum; m_i is the optical thickness of greenhouse substances absorbing thermal radiation within i-th spectral interval $\Delta\lambda_i$; h_i, σ_i and n_i are the height of the upper radiating layer, absorption cross-section and concentration of these greenhouse substances, respectively; F_{ei} is the radiative flux in i-th spectral interval outside the atmosphere. Note that generally $F_{ei}/F_e \neq \delta_i$. Variable b has the meaning of atmospheric transmissivity with respect to thermal radiation of the Earth's surface. The absolute value of greenhouse effect can be defined as the difference $F_s - F_e$.

In the atmosphere thermal radiation interacts with greenhouse substances that have concentrations not exceeding several fractions of per cent with respect to major air constituents. The cross-section of scattering of thermal radiation on absorption bands of triatomic molecules of greenhouse substances (H_2O, CO_2) is of resonance character, exceeding the cross-section of thermal radiation scattering on diatomic air molecules (N_2, O_2) (non-resonance Rayleigh scattering) by five-six orders of magnitude (Allen, 1955; Goody and Yung, 1989). In the process of resonance scattering the number of photons of a given wavelength remains constant, it is only the direction of their movement that changes. This leads to the condition of radiative equilibrium and energy balance for each absorption band of the greenhouse substances, which was used in derivation of Eq. (2.4).

If optical thickness m_i is of the same order of magnitude for all greenhouse substances, the upward flux of thermal radiation from the Earth's surface, F_s, increases infinitely with growing m_i, while transmissivity b tends to zero. If there are no absorbers in a certain n-th spectral interval, $m_n = 0$, there appears a so-called spectral window (Rodgers and Walshaw, 1966; Mitchell, 1989; Weaver and Ramanathan, 1995). In fact, a given spectral interval can be considered as a window when $m_n \ll m_i$ for all $i \neq n$. In the presence of a spectral window, increase in concentrations of the greenhouse substances with $i \neq n$ cannot lead to an infinite increase of the greenhouse effect. As follows from Eq. (2.4), the greenhouse effect is saturated at the following values of b and F_s (for $m_n = 0$): $b = \delta_n$, $F_s = F_e/\delta_n$. These limiting values have a clear physical explanation. The outgoing thermal flux F_e is fixed by the absorbed flux of solar radiation. As far as at $m_i \gg \delta_n^{-1}$ the atmosphere practically ceases to emit radiation into space in i-th spectral interval, i.e. $F_{ei} \to 0$, all the outgoing radiative flux passes into space through the spectral window directly from the surface, $F_e = \delta_n F_s$.

The third equation of (2.1) together with the boundary condition $F_1 = F_e$ can be re-written in the following form:

$$\begin{aligned} -\left[(F_{k-1} - F_k) - (F_k - F_{k+1})\right] &= 0 \\ F_k - F_{k-1} &= F_e \\ F_1 &= F_e \end{aligned} \tag{2.5}$$

A continuous analogue of the discrete number of a given layer, k, is the so-called optical depth τ:

$$\tau \equiv \int_z^\infty \frac{dz}{l(z)}, \qquad m \equiv \tau_s = \int_0^\infty \frac{dz}{l(z)}, \tag{2.6}$$

where $l(z)$ is the mean free path length of thermal photons at height z, τ_s is the optical thickness of the atmosphere.

For the upwelling flux of thermal radiation scaled by F_e, $f(\tau) \equiv F^+(\tau)/F_e \equiv F_k/F_e$, one can re-write Eq. (2.5) in the continuous representation as

$$\begin{aligned} -\frac{d^2 f(\tau)}{d^2\tau} &= 0 \\ \frac{df(\tau)}{d\tau} &= 1 \\ f(0) &= 1\,. \end{aligned} \tag{2.7}$$

Solution of Eq. (2.7) at the surface, $\tau = \tau_s$, is

$$f(\tau_s) = 1 + \tau_s\,. \tag{2.8}$$

As follows from Eq. (2.8), the absolute greenhouse effect, $F_s - F_e$, grows directly proportionally to the atmospheric thickness τ_s. We will now compare this result with solutions of the exact radiative transfer equation for different values of τ.

3 Analysis of the radiative transfer equation

In the planar three-dimensional case the stationary equation for transfer of radiation of a given wave length at height z has the form (Michalas and Michalas, 1984; Goody and Yung, 1989):

$$\mu \frac{\partial I(\mu, z)}{\partial z} = -\frac{1}{l(z)} I(\mu, z) + \frac{S(z)}{l(z)}, \tag{3.1}$$

where $I(\mu, z)$ is the radiation intensity, defined as the mathematical limit of energy transported per unit time in a given direction $\boldsymbol{n}$ through unit perpendicular area at height z by a bundle of rays propagating within a fixed unit solid angle, when the solid angle where measurements are taken tends to zero (Milne, 1930, p. 72); μ is the cosine between the given direction $\boldsymbol{n}$ and the vertical axis z, $S(z)$, the source function, is the radiative energy emitted per unit time in a cylinder of unit cross-section and length

equal to the mean free path length $l(z)$. Function $S(z)$ is assumed to be isotropic, i.e. μ-independent. The first term in the right-hand part of Eq. (3.1) describes absorption of radiation in the corresponding volume, the second one describes emission of radiation within the same volume. Thus, similar to Eqs. (2.1), Eq. (3.1) is based on the law of energy conservation: change in the energy of the ray, $\partial I(\mu,z)$, as the ray travels path $\partial s = \partial z/\mu$, is equal to the difference between the amounts of radiation absorbed and emitted by the matter along that path.

For the purposes of this paper we need to consider the radiation flux F and the energy density E, i.e. variables that are obtained from Eq. (3.1) by integrating it over solid angle, which, in the planar case considered, corresponds to integrating over μ. In the case of radiative equilibrium (absence of energy exchange between the matter and radiation) F and E are related to intensity (Eq. 3.1) as follows:

$$
\begin{aligned}
& Ec/4\pi \equiv J, \;\; F/4\pi \equiv H \\
& S(z) \;=\; J(z) \equiv \frac{1}{2}\int_{-1}^{1} I(z,\mu)\, d\mu \\
& H(z) \equiv \frac{1}{2}\int_{-1}^{1} \mu\, I(z,\mu)\, d\mu \,.
\end{aligned}
\tag{3.2}
$$

In this section we will refer to the mathematically convenient variables J and H (so-called Eddington variables) as to the normalised energy density and normalised flux, respectively.

Straightforward integration of Eq. (3.1) over μ does not yield an equation constraining H and J. To obtain such an equation, it is needed to go over from the differential (Eq. 3.1) to integral equations (Chandrasekhar, 1950; Michalas and Michalas, 1984; Goody and Yung, 1989). We first replace in Eq. (3.1) height z by optical depth $\tau, d\tau / l(z) \equiv -d\tau$ (see Eq. 2.6). Multiplying then both parts of Eq. (3.1) by $e^{-\tau/\mu}$ (this factor represents the solution of the homogenous Eq. (3.1) at $S(z) = 0$) and grouping together the two intensity-dependent terms of Eq. (3.1) at the left-hand part of the equation, one obtains that the τ-derivative of the product $I(\mu,\tau)e^{-\tau/\mu}$ is equal to $J(\tau)e^{-\tau/\mu}$.

Then, one integrates both parts of the new equation over τ within the limits $\tau \le \tau' < \infty$ for $\mu > 0$ and within the limits $0 \le \tau' < \tau$ for $\mu < 0$, and takes into consideration the boundary conditions – absence of exponential growth of H and J at $\tau \to \infty$ for $\mu > 0$ and zero value of the intensity at $\tau = 0$ for $\mu < 0$. In the two relations for $\mu I(\tau,\mu)$ thus obtained, for $\mu > 0$ and for $\mu < 0$, one may further introduce new integration variables, $\tau' - \tau = \mu x$ for $\mu > 0$ and $\mu' = -\mu$ and $\tau' - \tau = \mu' x$ for $\mu = -\mu' < 0$, and integrate them taking into account (Eq. 3.2). Then, dropping the prime of the new integration variable μ', the following relations for $J(\tau)$ and $H(\tau)$ are obtained:

$$
\begin{aligned}
& J(\tau) = J^{+}(\tau) + J^{-}(\tau) \\
& H(\tau) = H^{+}(\tau) - H^{-}(\tau)
\end{aligned}
\tag{3.3a}
$$

$$
\begin{aligned}
& J^{+}(\tau) \equiv \frac{1}{2}\int_0^1 d\mu \int_0^{\infty} e^{-x}\, J(\tau+\mu x)\, dx \\
& J^{-}(\tau) \equiv \frac{1}{2}\int_0^1 d\mu \int_0^{\tau/\mu} e^{-x}\, J(\tau-\mu x)\, dx
\end{aligned}
\tag{3.3b}
$$

$$
\begin{aligned}
& H^{+}(\tau) \equiv \frac{1}{2}\int_0^1 \mu\, d\mu \int_0^{\infty} e^{-x}\, J(\tau+\mu x)\, dx \\
& H^{-}(\tau) \equiv \frac{1}{2}\int_0^1 \mu\, d\mu \int_0^{\tau/\mu} e^{-x}\, J(\tau-\mu x)\, dx
\end{aligned}
\tag{3.3c}
$$

$$
\frac{dH^{+}(\tau)}{d\tau} \;=\; \frac{dH^{-}(\tau)}{d\tau} \;=\; \frac{1}{2}\left[J^{+}(\tau) - J^{-}(\tau)\right]
\tag{3.3d}
$$

$$J^-(\tau = 0) = H^-(\tau = 0) = 0. \quad (3.3e)$$

where + and – refer to the normalised flux and energy density of upwelling and downwelling radiation, respectively. Equation (3.3d) can be obtained differentiating the integral part of Eq. (3.3c) over τ, using integration by parts and Eqs. (3.3a,b). Equations (3.3) are exact, with no approximations made. Integral Eqs. (3.3b), (3.3c) differ from the Schwarzchild-Milne equations (Michalas and Michalas, 1984) by replacement of variables inside the integrals. Due to the presence of the exponential term e^{-x} in integrals (3.3b), (3.3c), the major contribution into these integrals comes from the interval $\mu x \sim 1$ for all values of τ, including $\tau \gg 1$. This allows one to use Eqs. (3.3b), (3.3c) in determination of the assymptotic behaviour of J and H at $\tau \gg 1$.

The greenhouse effect is fully determined by the changes that the upwelling radiation flux $H^+(\tau)$ undergoes propagating from the Earth's surface ($\tau = \tau_s$) to the top of the atmosphere ($\tau = 0$). Thus, we are primarily interested in finding the dependence of $H^+(\tau)$ on τ from Eq. (3.3c).

It follows from Eq. (3.3d) that $dH(\tau)/d\tau = 0$ and, consequently, $H(\tau) = H = \text{const}$. Using Eqs. (3.3a,b,c) it can be shown that this condition can be only fulfilled if at large values of $\tau \gg 1$ the normalised energy density $J(\tau)$ grows proportionally to the first power of τ, i.e. if at $\tau \gg 1$ we have that $J(\tau) = c_J H\tau + o(\tau^{n-1})$, where $c_J = \text{const}$. Indeed, let us express $J(\tau)$ as $J(\tau) = c_J H\tau^n$, where n is an arbitrary power, and put this expression into the integrals (3.3c). The difference between two integrals (3.3c) makes $H(\tau)$. Expanding the integral terms $(\tau \pm \mu x)^n$ into the series of powers of τ, taking into account that $\mu x \sim 1$, summing the terms with equal power and performing the integration, one obtains the following leading term of the assymptotic expression for $H(\tau)$ at large τ: $H(\tau) = (c_J/3)H\tau^{n-1} + o(\tau^{n-3})$. From this we both derive the value of $c_J = 3$ and conclude that a constant non-zero value of $H(\tau)$ is only possible when $n = 1$. Thus, the assymptote of $J(\tau)$ at large τ is a straight line, $J(\tau) = 3H(\tau + C_H)$, where C_H is a constant. Hopf (1934) found the exact value of $C_H = 0.710$.

We are now able to evaluate $H^+(\tau)$ at $\tau \gg 1$. Putting the assymptotic expression for $J(\tau) = 3H(\tau + C_H)$ at $\tau \gg 1$ into the first equation of Eq. (3.3c) and performing the

elementary integration over μ and x, we obtain:

$$f(\tau) \equiv \frac{H^+(\tau)}{H} = \frac{3}{4}\tau + 1.033, \quad f'(\tau) = \frac{3}{4}, \quad \tau \gg 1. \quad (3.4)$$

Note that the constant term in Eq. (3.4) is greater than unity. It also follows from Eq. (3.3c) that $H^+(\tau) = J^+(\tau)/2$ for $\tau \gg 1$.

Let us now explore the behaviour of $f(\tau)$ at small τ, $\tau \ll 1$. From Eqs. (3.3a), (3.3d) and (3.3e) we have $[H^+(0)]' = \frac{1}{2}J(0)$. In the planar three-dimensional case, at $\tau = 0$ photons propagate isotropically into the upper hemisphere only. The squared velocity of photons at $\tau = 0$ is determined by the relation $c^2 = c_x^2 + c_y^2 + c_z^2 = 3c_z^2$, as far as all directions of movement of isotropically propagating photons are equally probable. We have therefore $c_z = c/\sqrt{3}$, which means that the flux F is related to energy density E as $F = Ec_z = Ec/\sqrt{3}$. Finally, we obtain from Eq. (3.2) that $J(0) = \sqrt{3}H$. Thus, $f'(0) = \sqrt{3}/2$. So in the region of small τ we have:

$$f(\tau) = 1 + \frac{\sqrt{3}}{2}\tau, \quad f'(\tau) = \frac{\sqrt{3}}{2}, \quad \tau \ll 1. \quad (3.5)$$

Using Eqs. (3.3d) and (3.3b), we can obtain the next term of expansion of $f(\tau)$ over τ at $\tau \ll 1$. Taking the first derivative of integrals (3.3b) over τ and integrating the resulting integrals by parts, we obtain $f(\tau) = 1 + \frac{\sqrt{3}}{2}\tau + \frac{\sqrt{3}}{4}\tau^2 \ln\frac{\tau}{\tau_0}$, where τ_0 is a constant of the order of unity. It is easy to see from this expression that at $\tau \ll 1$ the second derivative of $f(\tau)$ is negative due to the presence of the logarithmic term.

In the intermediate region of $\tau \sim 1$ function $f(\tau) \equiv H^+(\tau)/H$ does not allow for a simple analytical representation. Nevertheless, it is clear that within this region $f(\tau)$ does not differ significantly from its assymptotic values given by Eqs. (3.4) and (3.5). For all τ the first derivative of $f(\tau)$ remains positive, as far as $J^+(\tau) > J^-(\tau)$, (see Eq. 3.3d). Consequently, $f(\tau)$ increases monotonously approaching its assymptote (3.4), Fig. 2. It can be also concluded that $f(\tau)'$ is decreasing monotonously at all τ. Indeed, it is evident from the condition of monotonous growth of $f(\tau)$ at all τ and the above discussed

fact that $f''(\tau) < 0$ for $\tau \ll 1$, that $f''(\tau)$ remains negative for $\tau \gg 1$ as well, so that $f(\tau)$ approaches the assymptote (3.4) from below. In any intermediate region, $\tau \sim 1$, $f(\tau)''$ cannot become positive either. This follows from the consideration of space uniformity: there are no selected points in space where the curve $f(\tau)$ could twice change the sign of its bending, Fig. 2. Consequently, $f'(\tau)$ decreases monotonously from its value Eqs. (3.5) to (3.4), thus changing by 15%. The region $\tau \sim \tau_c$, where the switch from assymptotic behaviour (Eq. 3.5 to 3.4) approximately occurs, corresponds to the point of intersections of the corresponding assymptotic lines, from which we have $\tau_c = 0.28$, Fig. 2. We note that the monotonous decrease of $f'(\tau)$ is only possible due to the fact that the constant term in Eq. (3.4), 1.033, is greater than the constant term in Eq. (3.5), which is equal to unity. It is easy to see from Fig. 2 that if it were not the case, function $f(\tau)$ would have to bend at least once, approaching the assymptote at $\tau \gg 1$ from above.

Equations (3.4), (3.5) for the upwelling flux of thermal radiation at the surface, $\tau = \tau_s$, can be written as

$$f(\tau_s) = 1 + \widetilde{\tau}_s, \quad \widetilde{\tau}_s \equiv k_1 \tau_s, \tag{3.6}$$

where $3/4 \le k_1 \le \sqrt{3/4}$ for any τ_s, $0 \le \tau_s < \infty$. Note that in all cases, (cf. Eq. 3.4), Eq. (3.5), the coefficient at the first power of τ_s is less than unity, as discussed in Sect. 2. The 15% change that coefficient k_1 undergoes in the region $\tau_s \sim 0.28$, from $k_1 \approx 3/4$ at $\tau_s \gg 1$ to $k_1 \approx \sqrt{3/4}$ at $\tau_s \ll 1$, (see Fig. 2), is dictated by the change in the character of radiation propagation. At large values of optical depth τ the radiation propagates approximately equally into the upper and lower hemispheres ($H^+ \approx H^-$, $J^+ \approx J^- \approx 2H^\pm$), while at small τ the predominant direction is into the upper hemisphere only ($H^+ \gg H^-$, $J^+ \gg J^-$, $J^+ \approx \sqrt{3}H^+ \approx \sqrt{3}H$). Thus, the change in k_1 monitors the change in the relation between the upwelling flux H^+ and the energy density J.

In the planar three-dimensional case, formula (3.6) coincides with Eq. (2.8) if one allows for the effective increase of the mean free path length l (or the equal decrease of the optical depth τ) by about 20%, (see Eqs. 3.4 and 3.5). When this minor correc-

tion factor is specified, the results of Sect. 2 are in full agreement with those obtained from the radiative transfer equation. Due to its physical transparency and mathematical simplicity, the consideration presented in Sect. 2 allows one to easily evaluate the contribution into heat transfer of non-radiative heat fluxes, which is done in the next section.

4 An account of non-radiative heat fluxes

Non-radiative dynamic flux of heat in the atmosphere derives mainly from convective transport of latent heat of water vapor and internal energy of air molecules. The only way for this heat flux to be released into space is by means of excitation at its expense of an additional number of energy levels of molecules of greenhouse substances and subsequent emission of thermal photons by the excited molecules. Additional energy levels are excited when molecules of greenhouse substances collide with molecules of other air constituents.

Collisional excitation of greenhouse molecules may occur at all atmospheric layers. To take this process into account, one has to add to the first equation of (2.5) a positive term. For every k-th layer, this term is equal to the flux of thermal radiation that is added to this layer due to non-radiative excitation of molecules of greenhouse substances.

It is convenient to write this term as $a_k F_e$ with dimensionless coefficients $a_k > 0$ normalised by the condition $\sum_{k=1}^{m+1} a_k = 1$. Here $a_{m+1} \equiv \gamma_s$ represents the flux of radiative thermal energy coming into the atmosphere from the Earth's surface, $\gamma_s \equiv (F_{m+1} - F_m)/F_e$. At each layer the incoming flux of radiation consists now of three parts: radiation F_{k-1} and F_{k+1} coming from the lower and upper neigbouring layers and radiation $a_k F_e$, which emerges at this layer due to the non-radiative excitation of greenhouse molecules.

The normalising condition $\sum_{k=1}^{m+1} \alpha_k = 1$ can be obtained by summing the modified first equation of (2.5), $-[(F_{k-1} - F_k) - (F_k - F_{k+1})] = \alpha_k F_e$, for all layers including the surface, for which it assumes the form $F_{m+1} - F_m = \gamma_s F_e$. The physical content of the normalising

condition $\sum_{k=1}^{m+1} a_k = 1$ is that the initial flux of energy of thermal radiation at the Earth's surface, γ_s, is at every layer fed with additional energy fluxes originating from non-radiative sources. At the top of the atmosphere all non-radiative fluxes disappear, while the thermal radiative flux reaches the maximum value of thermal radiative flux outgoing into space, F_e, which in the stationary case is equal to the incoming flux of absorbed solar radiation.

The important condition $a_k > 0$ means that all the dynamic energy fluxes must be converted into the energy of thermal photons and not vice versa, which is a manifestation of the second law of thermodynamics. If the collisional excitation of the absorption bands of greenhouse substances were absent or negligibly small, the air temperature would be the same throughout the entire atmospheric column, coinciding with that of the Earth's surface. The brightness temperature in each spectral interval containing absorption bands of greenhouse substances coincides with the surface temperature at the surface and then decreases with height. This means that the population density of the excited states of greenhouse molecules decreases with height. If one now switches on collisional interaction, this will lead to excitation of additional molecules at the expense of thermal energy of the hotter air. As a result, the air temperature will drop, while the brightness temperature in the corresponding absorption intervals will increase. According to the second law of thermodynamics, thermal energy is transported from the hotter medium to the cooler, i.e. from air molecules to the absorption bands of the greenhouse substances, and not vice versa, which corresponds to $a_k > 0$. In a stationary state, loss of energy by air molecules due to collisional excitation of the absorption bands is compensated by the non-radiative energy fluxes of convection and latent heat.

To take non-radiative heat fluxes into account, Eqs. (2.7) and their solution (2.8) in the continuous form can be re-written as follows:

$$-\frac{d^2}{d\tau^2} f(\tau) = \alpha(\tau) \tag{4.1a}$$

$$\left.\frac{df}{d\tau}\right|_{\tau=0} = \gamma_s + \int_0^{\tau_s} \alpha(\tau) d\tau = 1, \quad \gamma_s \equiv \left.\frac{df}{d\tau}\right|_{\tau=\tau_s} \tag{4.1b}$$

$$f(0) = 1 \tag{4.1c}$$

$$f(\tau_s) = 1 + \gamma_s \tau_s + \int_0^{\tau_s} d\tau \int_{\tau}^{\tau_s} d\tau' \alpha(\tau'). \tag{4.1d}$$

Function $\alpha(\tau) > 0$ (the continuous analogue of dimensionless coefficients a_k) is the flux of the non-radiative excitation of molecules of greenhouse substances per one mean free path length of thermal photons. The normalising condition for dimensionless coefficients a_k takes the form (4.1b) of one of the two boundary conditions for (4.1a). Equations (4.1a) and (4.1d) are written for the case of one greenhouse substance and may be extended to the general case of several greenhouse substances, (see Eqs. 2.3 and 2.4).

It follows from Eqs. (4.1b) and (4.1d) that the non-radiative heat fluxes work to diminish the value of $f(\tau_s)$ and the greenhouse effect. However, even in the limiting case of $\gamma_s = 0$ (i.e. when the thermal flux from the Earth's surface is completely non-radiative), the greenhouse effect retains a non-zero value. This quite expected result is a manifestation of the fact that the convection itself arises only due to the presence of a non-zero greenhouse effect.

Using sum rule (4.1b), we can write the dependence of $f(\tau_s)$ on τ_s in the following form for any τ_s:

$$f(\tau_s) = 1 + \widetilde{\tau}_s, \quad \widetilde{\tau}_s \equiv k_2 \tau_s \tag{4.2}$$

$$k_2 = \gamma_s + \frac{1}{\tau_s} \int_0^{\tau_s} d\tau \int_{\tau}^{\tau_s} d\tau' \alpha(\tau')$$

$$0 \le \gamma_s \le k_2 \le 1. \tag{4.3}$$

Coefficient k_2 has the meaning of the mean rate of change of the upwelling flux of thermal radiation in the atmosphere, (see Eqs. 4.1b). It is easy to check that the sum rule (4.1b) gives $k_2 = 1 + o(\tau_s)$ for $\tau_s \ll 1$. At $\tau_s \gg 1$, the mean rate of thermal radiative flux change, k_2, remains to be bounded from below by a finite value, irrespectively of the value of γ_s. In other words, k_2 does not decrease proportionally to $1/\tau_s$. Such a decrease of k_2 could in principle take place if the upwelling radiative flux $f(\tau)$, while propagating through the atmosphere, underwent changes predominantly in a fixed interval $(\tau_2 - \tau_1)$, which would be independent of τ_s and did not increase with growth of the latter. Such a situation is, however, impossible. Convection in the atmosphere is represented by vertical transport of macroscopic air volumes. In the course of their movement, these air volumes expand and become cooler and, consequently, continuously perform thermodynamic work. This work is continuously converted into thermal radiation, which means that the upwelling radiative flux $f(\tau)$ undergoes changes by receiving feeding from non-radiative heat fluxes throughout the entire area of atmospheric column, where convective fluxes are present. Thus, k_2 remains of the order of unity for any values of τ_s, including $\tau_s \gg 1$. This means that Eqs. (2.1), (2.7) and their solutions (2.2), (2.8) are valid for the case of a non-zero convective energy transport, if one replaces $m = \tau_s$ by $\tilde{m} = \tilde{\tau}_s$. Such a replacement is equivalent to multiplying the mean free path length l by a constant factor greater than unity. This factor can be retrieved from experimental data. The account of convection retains therefore the linear dependence of $f(\tau_s) \equiv F_s/F_e$ on the optical thickness τ_s. It is only the slope of the corresponding line that is changed (diminished). This result is in agreement with the results of previous studies (see, e.g. work of Stephens and Greenwald, 1991a, and their Fig. 7).

We give here values of $f(\tau_s)$ for several model functions $\alpha(\tau)$ that conform to the sum rule (4.1b). For the case of uniform dissipation of the non-radiative fluxes at all layers, $\alpha(\tau) = \beta = (1 - \gamma_s)/\tau_s$, we have $f(\tau_s) = 1 + \tau_s(1 + \gamma_s)/2$. For the case when the dissipation of non-radiative fluxes is governed by a power law, $\alpha(\tau) = \beta(\tau_s - \tau)^{n-1}$, we have $\beta = (1-\gamma_s)n/\tau_s$ and $f(\tau_s) = 1+\tau_s(1+n\gamma_s)/(1+n)$. As far as $\alpha(\tau)$ cannot increase

with height, it is reasonable to assume that $n \leq 1$. For the case of the non-radiative dissipation exponentially decreasing with decreasing τ, $\alpha(\tau) = \beta \exp[-(\tau_s - \tau)/\tau_\alpha]$, we have $\beta = (1 - \gamma_s)/\tau_\alpha(1 - \exp[-\tau_s/\tau_\alpha])$ and $f(\tau_s) = 1 + \tau_s(1 + \gamma_s)/2$ for $\tau_s/\tau_\alpha \ll 1$ and $f(\tau_s) = 1 + \tau_s$ for $\tau_s/\tau_\alpha \gg 1$. In the latter case the account of convection does not have any impact on the result obtained in the absence of convection. This result is expected, because in the case of exponential decrease of convective fluxes with decreasing optical depth τ, the major part of dissipation takes place in the lower atmospheric layers, so that the major contribution into the integral (Eq. 4.3) comes from the interval $(\tau_s-\tau)/\tau_\alpha \sim 1$, i.e. $\tau_s-\tau \ll \tau_s$. In all other cases considered, the coefficient k_2 (Eq. 4.2) at the first power of τ_s changes by no more than twofold as compared to unity corresponding to the absence of convection.

The major result of Sects. 2, 3 and 4 is the linear proportionality, (cf. Eqs. 2.2, 2.8, 3.6, and 4.2), between the upwelling flux of thermal radiation at the Earth's surface, F_s, and the optical atmospheric thickness τ_s, i.e. ultimately between F_s and atmospheric concentrations of the greenhouse substances. The coefficient of this linear proportionality does not significantly differ from unity and can be derived from the experimental data. In the sections to follow we examine implications of this dependence for climate stability.

5 Stability of possible Earth's climates

Averaged over a sufficiently large area, the energy balance at the Earth's surface (including the atmosphere) has the form (North et al., 1981; Dickinson, 1985):

$$C\frac{dT}{dt} = F_{\text{in}} - F_{\text{out}} \equiv -\frac{dU}{dT}$$
$$F_{\text{in}} \equiv I_o a(T), \quad F_{\text{out}} \equiv \sigma_R T^4 b(T)\,. \tag{5.1}$$

Here T is the absolute temperature of the Earth's surface; C is the average heat capacity per unit surface area; F_{in} is the flux of short-wave solar radiation absorbed by

the Earth's surface, I_o is the total incoming flux of solar radiation outside the atmosphere, the global mean value of I_o is equal to $\overline{I_o} = I/4$, where $I = 1367\ \mathrm{Wm}^{-2}$ is the solar constant (Willson, 1984; Mitchell, 1989); $a(T) \equiv 1 - A(T)$ is the share of the incoming flux of solar radiation absorbed by the Earth's surface (coalbedo); $A(T)$ is the planetary albedo; F_{out} is the flux of long-wave thermal radiation leaving the planet into space; $\sigma_R = 5.67 \cdot 10^{-8}\ \mathrm{Wm}^{-2}\mathrm{K}^{-4}$, (see Eq. 2.3); $b(T)$ has been defined in Eq. (2.4); $U(T)$ is the potential (Liapunov) function. The only independent variable in Eq. (5.1) is temperature T.

In a stationary state, when the energy content does not change, $CdT/dt = 0$, the derivative of the potential function $U(T)$ turns to zero, and $U(T)$ has an extreme—maximum or minimum. The central part of Eq. (5.1) also turns to zero, thus determining a stationary temperature $T = T_s$:

$$I_o a(T_s) - \sigma_R T_s^4 b(T_s) = -\left.\frac{dU}{dT}\right|_{T=T_s} = 0$$

$$T_s = T_o \left(\frac{a(T_s)}{b(T_s)}\right)^{\frac{1}{4}}, \quad T_o \equiv \left(\frac{I_o}{\sigma_R}\right)^{\frac{1}{4}}, \overline{T_o} = \left(\frac{I}{4\sigma_R}\right)^{\frac{1}{4}}. \tag{5.2}$$

Here $\overline{T_o} = 278\,\mathrm{K}$ is the orbital temperature. The second derivative of the potential function $U(T)$, W, determines the character of the extreme. It is a stable minimum when $W > 0$, and an unstable maximum when $W < 0$.

$$W \equiv \left(\frac{d^2U}{dT^2}\right)_{T=T_s} = \frac{I}{4}\left(\frac{a(T)}{T}(4 + \beta - \alpha)\right)_{T=T_s}$$

$$\alpha \equiv \frac{da}{dT}\frac{T}{a}, \quad \beta \equiv \frac{db}{dT}\frac{T}{b}. \tag{5.3}$$

The stationary state is stable at $\alpha - \beta < 4$ and unstable at $\alpha - \beta > 4$. In particular, stationary states in the regions of slowly changing, practically constant a and b, for which $\alpha \ll 4$ and $\beta \ll 4$, are stable.

On Earth the major greenhouse substances are the water vapour and carbon dioxide. The existing spectral windows remain transparent at clear sky and are "closed" with appearance of clouds. For the terrestrial atmosphere the transmissivity b (Eq. 2.4) can be written as

$$b = \frac{\delta_{\mathrm{H_2O}}}{\widetilde{m}_0 + \widetilde{m}_{\mathrm{H_2O}} + 1} + \frac{\delta_{\mathrm{CO_2}}}{\widetilde{m}_0 + \widetilde{m}_{\mathrm{CO_2}} + 1} + \frac{\delta_0}{\widetilde{m}_0 + 1}, \tag{5.4}$$

where $\delta_{\mathrm{H_2O}}$ and $\delta_{\mathrm{CO_2}}$ are the relative spectral intervals, (see Eq. 2.3), that contain the major absorption bands of water vapour (H_2O) and CO_2; δ_0 is the relative spectral interval which corresponds to spectral windows that are closed by the cloudiness. Using Eq. (2.3) we estimate the relative spectral intervals $\delta_{\mathrm{CO_2}}$, δ_0 and $\delta_{\mathrm{H_2O}}$ as follows:

$$\delta_{\mathrm{CO_2}} = 0.19, \quad \delta_0 = 0.25, \quad \delta_{\mathrm{H_2O}} = 0.56, \quad \sum_i \delta_i = 1. \tag{5.5}$$

The value of $\delta_{\mathrm{CO_2}}$ is calculated for the major absorption band of CO_2 centered at 15 μm and extending from 13 μm to 17 μm (Rodgers and Walshaw, 1966). The atmospheric spectral window spreads from 8 μm to 12 μm. Its value (Eq. 5.5) approximately coincides with the estimate given by Weaver and Ramanathan (1995). The absorption area of H_2O, located at different parts of the thermal spectrum, is calculated from the condition $\sum_i \delta_i = 1$.

The effective optical thickness $\widetilde{m}_i$ in Eq. (5.4) is estimated as the relative difference between the upward fluxes of thermal radiation in the corresponding spectral interval at the Earth's surface, F_{si}^+, and outside the atmosphere, F_{ei}^+, (see Eqs. 2.2, 3.6, and 4.2):

$$\widetilde{m}_i = k m_i = (F_{si}^+ - F_{ei}^+)/F_{ei}^+, \quad m_i = h_i n_i \sigma_i,$$

$$F_{si}^+ = \int_{\lambda_1}^{\lambda_2} I_p(\lambda, T_s)d\lambda, \quad F_{ei}^+ = \int_{\lambda_1}^{\lambda_2} I_p(\lambda, T_{ei})d\lambda \tag{5.6}$$

where $\lambda_2 - \lambda_1 = \Delta\lambda_i$ is the spectral interval of wavelengths, which defines the value of δ_i as described in Eq. (2.3); $I_P(\lambda, T)$ is the Planck function, T_{ei} is the brightness temperature in the spectral interval $\Delta\lambda_i$ outside the atmosphere; n_i and σ_i are the absorption cross-section and concentration of i-th greenhouse substance, respectively; h_i is the height of a homogeneous atmosphere where the corresponding greenhouse substance would be evenly distributed. In calculation of F_{ei}^+ the use of Planck function is not indispendable. It is employed here for convenient determination of the brightness temperature only. One could obtain F_{ei}^+ by direct integration of the spectral distribution of the outgoing thermal flux outside the atmosphere.

The relative absorption intervals δ_{CO_2}, δ_0 and δ_{H_2O} include contributions from other greenhouse gases. For instance, the relative absorption interval δ_{CO_2} contains weak absorption bands of H_2O, while δ_0 contains absorption bands of O_3 and the so-called continuum absorption spectrum of H_2O (Rodgers and Walshaw, 1966; Goody and Yung, 1989). However, the optical thickness m_k corresponding to these weak absorption bands is small compared to the corresponding value m_i of the major greenhouse substances in the interval considered, $m_k \ll m_i$. Thus, such m_k were neglected in Eq. (5.4).

As shown in Sects. 2–4, the effective optical thickness $\tilde{m}_i$ (Eq. 5.6) differs from the optical thickness m_i, defined with use of the mean free path length, (see Eq. 2.4), by a multiplier $k \sim 1$ ($0.5 < k < 1$). This multiplier accounts both for the non-radiative heat fluxes and the divergence of rays in the three-dimensional atmosphere. The most important feature of Eq. (5.6) is the direct proportionality between m_i (and, consequently, $\tilde{m}_i$) and the total mass $h_i n_i$ of i-th greenhouse substance in the atmospheric column.

To construct the dependence of the global transmissivity function b on surface temperature T we will assume that, in accordance with observations, the modern global mean surface temperature $T_s = 288$ K (15°C) is stationary, thus conforming to Eq. (5.2). Using Eq. (5.6), we determine the modern value of $\tilde{m}_{CO_2}$ from the directly measured values of $F_{sCO_2}^+$ and $F_{eCO_2}^+$ (Conrath et al., 1970; Goody and Yung, 1989, p. 219). It gives (the brightness temperature of the 15 μm CO_2 band outside the atmosphere is

about 220 K):

$$\tilde{m}_{CO_2} = 1.9 \tag{5.7}$$

Value of $b(T_s)$ in the stationary point $T_s = 288$ K is determined from Eq. (5.2) using the observed value of coalbedo $a(T_s) = 0.70$ (Mitchell, 1989) and the observed value of orbital Earth's temperature $\overline{T_o}$ (Eq. 5.2). These values give $b(T_s) = 0.61$.

The relative contribution of clouds, d, into the global absolute greenhouse effect $F_s - F_e$ is about 18%, $d = 0.18$ (Raval and Ramanathan, 1989; Stephens and Greenwald, 1991b). Accordingly, the global value of b for the clear sky is equal to $b_{cs} = F_{ecs}/F_s = (F_e + (F_s - F_e)d)/F_s = 0.68$, where $F_{ecs} > F_e$ is the outgoing flux of thermal radiation outside the atmosphere in the absence of clouds. Absence of clouds corresponds to $\tilde{m}_0 = 0$ in Eq. (5.4). Setting in Eq. (5.4) $\tilde{m}_0 = 0$, $b = b_{cs} = 0.68$ and $\tilde{m}_{CO_2} = 1.9$ (Eq. 5.7) and taking into account Eq. (5.5), we obtain

$$\tilde{m}_{H_2O}(T_s) = 0.53. \tag{5.8}$$

Finally, using estimates (5.7) and (5.8) in Eq. (5.4) for the global value of $b(T_s) = 0.61$, we obtain from Eq. (5.4) the following value of $\tilde{m}_0$:

$$\tilde{m}_0(T_s) = 0.15, \quad r \equiv \tilde{m}_0/\tilde{m}_{H_2O} = 0.29. \tag{5.9}$$

The values of $\tilde{m}_i$ (Eq. 5.7 to 5.9) are derived from observations and take therefore into account the contributions into heat transfer of the non-radiative thermal fluxes, see Sect. 4.

Near-surface concentration of the water vapour changes proportionally to the saturated concentration, which grows exponentially with increasing temperature in accordance with the Clausius-Clapeyron formula (see, e.g. Raval and Ramanathan, 1989; Nakajima et al., 1992):

$$\widetilde{m}_{H_2O}(T) = \exp\left(\varepsilon - \frac{T_{H_2O}}{T}\right)$$

$$T_{H_2O} \equiv \frac{Q_{H_2O}}{R} = 5.3 \cdot 10^3 \mathrm{K}, \quad \varepsilon = 17.76\,, \tag{5.10}$$

where ε is determined from Eq. (5.8).

Due to the finite mass of the Earth's hydrosphere, the greenhouse effect on Earth cannot grow – while b cannot diminish – infinitely with growing surface temperature. This can be taken into account by stopping the growth of $\widetilde{m}_{H_2O}(T)$, when $b(T)$ reaches a certain minimum value $b_{min} = 0.01$. The value of b_{min} is chosen equal to the corresponding value of b on Venus, where the atmospheric pressure is of the same order of magnitude as it would be on Earth were its hydrosphere evaporate (Pollack et al., 1980; Mitchell, 1989). We assume also that the ratio between atmospheric concentrations of liquid water and water vapour remains constant over a sufficiently broad temperature interval, so that r in Eq. (5.9) can be held temperature-independent. Thus, we arrive at the following expression for $b(T)$ (Fig. 3):

$$b(T) = \frac{0.56}{1.29\varphi(T) + 1} + \frac{0.19}{0.29\varphi(T) + 2.9} + \frac{0.25}{0.29\varphi(T) + 1}\,, \quad T \le 422\,\mathrm{K}\,;$$

$$b(T) = 0.01\,, \qquad T \ge 422\,\mathrm{K}\,;$$

$$\varphi(T) \equiv \exp\left(17.76 - \frac{5.3 \cdot 10^3}{T}\right)\,. \tag{5.11}$$

At the modern value of the global mean surface temperature $T_s = 15^\circ$C the coalbedo function approaches its maximum value (North et al., 1981). At colder temperatures, with increasing degree of the planet's glaciation, the coalbedo diminishes, while the albedo $A(T)$ starts to grow. This growth is limited from above by the value $A_{max} \sim 0.7$ ($a_{min} \sim 0.3$), which characterises the reflectivity of snow cover (Hibler, 1985). With rising surface temperature, $T > 15^\circ$C, accompanied by evaporation of water, the albedo

should increase as well due to the growing cloudiness and increasing atmospheric density. This is in agreement with the known high value of albedo on Venus, where $A \sim 0.75$ (Mitchell, 1989), which approximately coincides with $A_{max} \sim 0.7$ for an ice-covered Earth. Modern climate sensitivity with respect to temperature-dependent changes in albedo, $\lambda_A \equiv -F_s a'(288\,\mathrm{K})$, is of the order of $-(0.3 \div 0.8)\ \mathrm{Wm^{-2}K^{-1}}$ (Dickinson, 1985). This allows one to conclude that the modern value of coalbedo is located to the left – along the T axis – from its maximum possible value (were the modern coalbedo coincide with the maximum, the climate sensitivity λ_A, which is proportional to the temperature derivative of coalbedo, would be equal to zero). To take into account these physically transparent properties of coalbedo, we choose function $a(T)$ in the form of a Gaussian curve (Fig. 4). The location of the maximum is specified by the assumption that the global ice shield completely disappears when the global mean surface temperature rises up to 295 K (22°C). The modern albedo of Earth is equal to 0.30, where 0.25 falls on reflectivity of short-wave radiation by the atmosphere and 0.05 (one sixth part) is attributed to reflectivity by the Earth's surface, including the oceans (Schneider, 1989; Mitchell, 1989). Assuming that the global snow cover occupies about 5% of the total Earth's surface and taking the global mean albedo of the Earth's surface in the absence of clouds equal to ~0.1 (Ramanathan and Coakley, 1978) and the albedo of snow about ~0.7 (Hibler, 1985), we find that melting of the global snow cover will decrease the planetary albedo by $(0.7 - 0.1) \times 0.05 \times (1/6) \sim 5 \cdot 10^{-3}$. Thus, we put $a_{max} = a(295\,\mathrm{K}) = 0.705$ and $a(288\,\mathrm{K}) = 0.70$. The characteristic width of the Gaussian curve is specified by the average value of modern climate sensitivity to albedo, $\lambda_A \sim -0.6\,\mathrm{Wm^{-2}K^{-1}}$ (Dickinson, 1985) at $T_s = 288$ K. Finally, we take $a_{min} = 0.3$ for the assymptotic values of the Gaussian curve at large and low temperatures. We thus arrive at the following expression for $a(T)$ (Fig. 4):

$$a(T) = 0.30 + 0.405 \exp\left[-\left(\frac{T - 295\,\mathrm{K}}{60\,\mathrm{K}}\right)\right] \tag{5.12}$$

Formulas (5.11) and (5.12) allow for a unambiguous derivation of the potential function $U(T)$ (Eq. 5.1), Fig. 5. Integration constant in Fig. 5 is chosen such that the value of

$U(T)$ in the point of the right extreme, $T = 652$ K, is equal to zero.

As is clear from Fig. 5, there are only two physically stable states of the Earth's climate. These are the state of complete glaciation of the Earth's surface **1** and complete evaporation of the hydrosphere **3**. The intermediate stationary state **2** which corresponds to the maximum of the potential function $U(T)$ is physically unstable.

In accordance with Boltzmann distribution, height of the homogeneous atmosphere, h_i (Eq. 5.6), grows proportionally to the temperature of the Earth's surface. The atmospheric concentration of water vapour near the surface is determined by the equilibrium between the water vapour and liquid water of the global oceans and terrestrial vegetation. Thus, the total amount of water vapour in the atmospheric column, $h_{H_2O} n_{H_2O}$, and its optical thickness increase due to temperature dependences of both h_{H_2O} and n_{H_2O}. Surface temperature is related to the upward flux of thermal radiation of the surface by the Stephen-Boltzmann formula, $F_s^+ = \sigma_R T^4$. Thus, at large $\widetilde{m}_i \gg 1$ we have from Eq. (5.6) that $h_i \propto (F_{si}^+)^{1/4} \propto (h_i n_i \sigma_i)^{1/4}$, so that $h_i \propto (n_i \sigma_i)^{1/3}$ and $\widetilde{m}_i \propto (n_i \sigma_i)^{4/3}$. In Eq. (5.11) we have neglected the additional acceleration in growth of $\widetilde{m}_{H_2O}$ due to the dependence of h_{H_2O} on n_{H_2O}. Accounting for this dependence leads to substitution of $T_{H_2O} = 5.3 \cdot 10^3$ K in Eq. (5.10) by $T_{H_2O} = 7.1 \cdot 10^3$ K. This will only increase the rate of $b(T)$ change with changing temperature, thus enhancing the physical instability of the modern climate, (see Eq. 5.3).

The right ordinate axis in Fig. 5 shows $U(T)$ scaled by the value of the global mean flux of the incoming solar radiation $\overline{I_o} = I/4 = 342$ Wm^{-2}. In terms of $\overline{I_o}$, the depth of the potential pit **3** corresponding to the stable state of complete evaporation of the hydrosphere, is equal to 58 K, while the depth of the potential pit **1** corresponding to complete glaciation is equal to 1.3 K. The latter value coincide by the order of magnitude with the depth of the glaciation potential pit obtained by North et al. (1981), where it constituted ∼4 K. Besides the differences in the transmissivity functions $b(T)$ employed, the difference in the depth of pits is explained by a larger value of climate sensitivity $\lambda_A = -0.8$ Wm^{-2}K^{-1} used by North et al. (1981) as compared to the average value of $\lambda_A = -0.6$ Wm^{-2}K^{-1} (Dickinson, 1985) accepted by us. The locations of glaciation pits

approximately coincide, −37°C and −43°C in the work of North et al. (1981) and the present paper, respectively.

The stable state **1** of complete glaciation of the Earth's surface was previously investigated under the assumption of a linear dependence of F_{out} (Eq. 5.1) on temperature in the whole interval of temperatures considered (Ghil, 1976; North and Coakley, 1979; North et al., 1981). The stability of this state was discussed in the context of possible changes in the solar constant I. The stable state **3** of complete evaporation of the hydrosphere arises due to the fact that the hydrosphere has a finite mass and the transmissivity function $b(T)$ is therefore limited from below by $b = b_{min} > 0$. In the absence of this limitation the greenhouse effect and the surface temperature might increase infinitely. This phenomenon is called "runaway" greenhouse effect and was also extensively discussed in the literature (Ingersoll, 1969; Rasool and de Berg, 1970; Nakajima et al., 1992; Weaver and Ramanathan, 1995).

In the state of complete evaporation of the hydrosphere, the surface temperature (∼ 700 K) and atmospheric pressure (∼ 300 bars) are such that the atmospheric water finds itself above the critical point, where the difference between gas and liquid disappears. The major constituent of the atmosphere of Venus, CO_2, is also above the critical point there. Another feature of dense atmospheres is that the incoming solar radiation is absorbed predominantly in the upper atmospheric layers, with little reaching the planet's surface (Rossow, 1985). Both these features are approximately taken into account by setting the limiting value of the transmissivity function b_{min} equal to the corresponding value on Venus. We do not aim at exact determination of the stationary value of global mean surface temperature in state **3**. We only assert that this stable state exists, similar to what is found on Venus.

Stable states **1** and **3** arise due to the practical constancy of the transmissivity function b and the coalbedo a in the considered intervals of high and low temperatures, (see Eq. 5.3 and Figs. 3, 4). This, in its turn, is caused by the constancy in the aggregate phase of the major greenhouse constituent – the hydrosphere is solid in state **1** and gaseous in state **3**. The two minima of the potential function, Fig. 5a, can be joined

by a continuous curve only via an unstable maximum in the temperature interval corresponding to the liquid hydrosphere. There are no physical reasons for appearance of a third minimum, which would be inevitably accompanied by two additional maxima in Fig. 5. Formation of such structures would have pointed to the existences of singularities in the temperature-dependent behaviour of a and b in the vicinity of the modern global mean surface temperature. These singularities should have had a clear physical interpretation, just as do the stable minima **1** and **3**.

Transition from the state **1** to state **3** is accompanied by nearly a hundredfold monotonouse decrease of $b(T)$, as compared to no more than a threefold change of coalbedo $a(T)$. Thus, despite that the exact temperature-dependent behaviour of coalbedo remains to a large extent unknown, it seems unlikely that any plausible assumptions about $a(T)$ may significantly change the behaviour of $U(T)$, Fig. 5, leading to appearance of singularities of $U(T)$ in the vicinity of $T = 15^{\circ}$C.

We determined our single parameter, constant ε in Eq. (5.10), demanding that the modern global mean surface temperature is stationary. In a stationary unstable state, where the curves $F_{\text{in}}(T)$ and $F_{\text{out}}(T)$ intersect, (see Eq. 5.1), the temperature derivative of $F_{\text{in}}(T)$ is larger than that of $F_{\text{out}}(T)$ (see Fig. 6). A characteristic feature of such a state is that if $F_{\text{in}}(T)$ were to decrease, the unstable stationary temperature would become larger, and vice versa. A colder stationary unstable climate arises at larger global mean values of the absorbed solar radiation $F_{\text{in}} = Ia/4$. If function $a(T)$ is held unchanged, it corresponds to an upward shift of the curve $F_{\text{in}}(T)$, Fig. 6, without altering its form. At large values of a or I, the curve $F_{\text{out}}(T)$ may remain below the curve $F_{\text{in}}(T)$ at all T excluding very large ones. The stationary intersection points **1** and **2** will then disappear, and the only stationary stable state will be the gaseous hydrosphere, **3**, which corresponds to the runaway greenhouse effect.

Generally, functions $a(T)$, $b(T)$ and $F_{\text{out}}(T) \equiv \sigma_R T^4 b(T)$, constructed on the basis of well-established physical laws for a given type of planetary surface, e.g. oceanic, should be valid for description of all local areas of the same surface type. These areas differ from each other by the annual values of the incoming solar flux I_o (Eq. 5.1). At

the modern global mean surface temperature, $T_s = 288$ K, $F_{\text{out}}(T)$ approaches maximum, Fig. 6. It follows that in the equatorial oceanic regions, where the incoming solar flux is considerably larger than the global average, the regional value of $F_{\text{in}}(T)$ would be larger than the maximum possible value of $F_{\text{out}}(T)$. The unstable stationary state will disappear, driving the equatorial regions to a state of runaway greenhouse effect. Thus, even if a given value of the global mean surface temperature corresponds to a stationary unstable state, as determined by $a(T)$ and $b(T)$, (see Eq. 5.3), this does not by itself guarantee unstable stationarity for all local areas of the the planetary surface.

6 Stability of the modern climate

The existence of life during the last several billion years, together with other paleodata (Savin, 1977; Watts, 1982; Berggren and Van Couvering, 1986), indicates that the modern Earth's climate is stable. It means that in the vicinity of the modern mean global surface temperature, the behaviour of $a(T)$ and $b(T)$ differs from Eqs. (5.11) and (5.12).

A stable state arises when in the point where $F_{\text{out}}(T)$ and $F_{\text{in}}(T)$ intersect, the temperature derivative of $F_{\text{out}}(T)$ is larger than that of $F_{\text{in}}(T)$. In particular, the nearest to absolute zero extreme of $U(T)$ is always stable (see Figs. 5 and 6). Indeed, $F_{\text{out}}(0) = 0$, while $F_{\text{in}}(0) > 0$. Therefore, $F_{\text{out}}(T)$ will cross $F_{\text{in}}(T)$ from below, if only its slope is steeper than that of $F_{\text{in}}(T)$.

If the greenhouse effect is completely absent or temperature-independent ($b(T) = \text{const}$), there is only one point of intersection between $F_{\text{out}}(T)$ and $F_{\text{in}}(T)$, and it is stable. The second, unstable, point of intersection will arise, if the decrease in $b(T)$ with temperature compensates the growth proportional to T^4, $F_{\text{out}}(T) \equiv b(T)\sigma_R T^4$, so that the derivative of $F_{\text{out}}(T)$ becomes less than that of $F_{\text{in}}(T)$. Due to the existing physically transparent limitations $0.3 \le a(T) \le 0.7$, (see Eq. 5.12), at $b(T) = \text{const}$ no changes in coalbedo $a(T)$ are able compensate the growth of $F_{\text{out}}(T) \propto \sigma_R T^4$ and create a second point of intersection between $F_{\text{out}}(T)$ and $F_{\text{in}}(T)$.

For a stable intersection point to appear in the vicinity of $T \sim 15^{\circ}$C, it is necessary that the curve $F_{out}(T)$ makes here a zigzag, with three points of intersections with $F_{in}(T)$, of which two are unstable and one is stable (see Fig. 7b). In the central part of this zigzag function $b(T)$ is approximately constant, so that the curve $F_{out}(T)$ crosses $F_{in}(T)$ from below, just as in the absence of the greenhouse effect ($b = 1$), but at higher values of temperature. Thus, generating the zigzag of $F_{out}(T)$ and choosing the value of $b < 1$, it is possible to form a stationary stable state in the region of life-compatible temperatures. Within the central part of this zigzag, the derivative of $F_{out}(T)$ is large than that of $F_{in}(T)$. The stable intersection point can therefore move to the right and to the left in response to regional changes in the incoming solar flux I_o. Thus, stable stationary states can form in the regions with lower (polar) and higher (equatorial) temperatures as compared to the global average.

The temperature-dependent behaviour of $b(T)$ in the vicinity of the modern value of global mean surface temperature can be derived from observations. As shown in numerous studies (Budyko, 1969; North and Coakley, 1979; North et al., 1981; Raval and Ramanathan, 1989; Stephens and Greenwald, 1991a,b), the regional function $b(T)$ remains an approximately linear function of temperature within a broad temperature interval. The gentle slope of this almost constant function ensures a stable stationary state of the modern climate for all physically plausible functions $a(T)$. As the mean value of a linear function coincides with its value of the mean argument, one can assume that measurements of $b(T)$ in different regions and at different temperatures describe the temperature-dependent behaviour of the global mean function $b(T)$.

The observed greenhouse effect dependence on temperature within the temperature interval from $\sim 0^{\circ}$C (273 K) to $\sim 30^{\circ}$C (303 K) was described by Raval and Ramanathan (1989) and Stephens and Greenwald (1991b) for clear and cloudy sky, respectively. Quantitatively, the obtained results can be summarised as follows, Fig. 7a: For 273 K $\leq T \leq$ 299 K:

$$b_{RR}(T) = 0.67 - 2.6 \cdot 10^{-3} \times (T - 288) \tag{6.1a}$$

$$b_{SG}(T) = 0.59 \tag{6.1b}$$

For 299 K $\leq T \leq$ 303 K:

$$b_{RR}(T) = 0.64 - 9.6 \cdot 10^{-3} \times (T - 299) \tag{6.2a}$$

$$b_{SG}(T) = 0.59 - 85.5 \cdot 10^{-3} \times (T - 299). \tag{6.2b}$$

Function $b_{RR}(T)$ is obtained by us by linear approximation of the point measurements of $B_{RR}(T) \equiv 1 - b_{RR}(T)$ presented in Fig. 2 of the work of Raval and Ramanathan (1989). The approximation was performed separately for temperature intervals 273 K $\leq T \leq$ 299 K and 299 K $\leq T \leq$ 303 K. The correlation coefficient equals 0.784 ($\sim$ 1500 d.f.) and 0.653 ($\sim$ 500 d.f.) for the curves (6.1a) and (6.2a), respectively. According to Stephens and Greenwald (1991b), the value $1/b_{SG}(T)$ remains approximately equal to 1.7 in the temperature interval from 275 K to 301 K and starts to rise rapidly at T = 299 K reaching 2.4 at T = 301 K. Function $b_{SG}(T)$ (Eq. 6.1b to 6.2b) reflects this behaviour.

As follows from comparison of Eqs. (6.1) and (6.2), the observed temperature-dependent behaviour of transmissivity functions $b_{RR}(T)$ and $b_{SG}(T)$ differ significantly from the physical behaviour (Eq. 5.11) in the interval from 0°C to 26°C (see Eq. 6.1). At $T > 26^{\circ}$C both functions undergo drastic changes (which was noted by both Raval and Ramanathan, 1989, and Stephens and Greenwald, 1991b) and approach the physical behaviour (Eq. 5.11) in the interval from 26°C to 30°C. The slope of $b_{RR}(T)$ in this interval exactly coincides with that of Eq. (5.11). The slope of $b_{SG}(T)$ is about ten times steeper (Fig. 7a).

As far as $b_{RR}(T)$ describes clear sky and $b_{SG}(T)$ – cloudy sky only, the corresponding curves, Fig. 7a, lie above and below the global mean value b(288 K) = 0.61, respectively. The true empirical curve $b_{emp}(T)$, corresponding to mean cloudiness, goes between the curves $b_{RR}(T)$ and $b_{SG}(T)$. Taking mean global cloudiness of about 50% (Rennó et al., 1994), we have

$$b_{\mathrm{emp}}(T) = \frac{b_{\mathrm{RR}}(T) + b_{\mathrm{SG}}(T)}{2} =$$
$$= \begin{cases} 0.63 - 1.3 \cdot 10^{-3} \times (T - 288), & 273\,\mathrm{K} \le T \le 299\,\mathrm{K} \\ 0.62 - 47.6 \cdot 10^{-3} \times (T - 299), & 299\,\mathrm{K} \le T \le 303\,\mathrm{K} \end{cases} \tag{6.3}$$

We note that $b_{\mathrm{emp}}(288\ \mathrm{K}) = 0.63$, which only slightly differs from the global value of $b(288\ \mathrm{K}) = 0.61$, thus justifying the applied procedure for derivation of $b_{\mathrm{emp}}(T)$.

At $T = 273$ K function $b_{\mathrm{emp}}(T)$ (6.3) coincides with function $b_{\mathrm{NC}}(T)$, used in the work of North and Coakley (1979) and North et al. (1981), which was constructed on the basis of a linear dependence of F_{out} on temperature, $F_{\mathrm{out}}(T) \equiv b_{\mathrm{NC}}(T)\sigma_R T^4 = [203.3 + 2.09 \times (T - 273)]\ \mathrm{Wm}^{-2}$. At $T = 234$ K (-39°C) function $b_{\mathrm{NC}}(T)$ thus defined starts to diminish with further decrease of temperature and becomes negative at $T \le 276$ K (-97°C). Such a behaviour is physically unjustified, as far as with decreasing temperature the transmissivity function $b(T)$ should increase monotonously, Fig. 3, governed by the diminishing amount of the major greenhouse substances (water and clouds) in the atmosphere. At $T \to 0$ K the linear dependence $b_{\mathrm{RR}}(T)$ yields a physically meaningless value greater than unity. Constancy of $b_{\mathrm{SG}}(T)$ at $T \to 0$ K is physically implausible as well: as far as with decreasing temperature the atmospheric water content, including liquid water, is diminishing, the greenhouse effect of cloudy sky should also change.

It follows that the real behaviour of $b_{\mathrm{emp}}(T)$ at certain $T < 273$ K differs considerably from Eq. (6.3) and approaches the physically sensible assymptotic values described by Eq. (5.11), Fig. 3, similar to its behaviour at higher temperatures, (see Eqs. 6.2a and 6.2b). The unknown behaviour of $b_{\mathrm{emp}}(T)$ at $T < 273$ K is represented in Fig. 7a by dashed line. Intersections of $b_{\mathrm{emp}}(T)$ with the physical function $b(T)$ (Eq. 5.11) occur at $T = 266$ K and $T = 302$ K. The slope of the model dashed line $b_{\mathrm{emp}}(T)$ at $266\mathrm{K} \le T \le 273$ K is taken arbitrarily to equal one half of the slope of $b_{\mathrm{emp}}(T)$ at $299\ \mathrm{K} \le T \le 303$ K.

It is important to note that when the behaviour of the regional functions $b(T)$ deviates from the linearity observed in the vicinity of the mean global temperature, (cf. Eqs. 6.1 and 6.2), the global function $b(T)$ will be better described by those regional functions that correspond to the largest areas of the Earth's surface. For example, the modern regional function $b(T)$ corresponding to low latitudes, i.e. extensive equatorial territories with high temperatures ($T > 20^{\circ}$C), should describe the behaviour of global function $b(T)$ at high temperatures better than the modern high-latitude regional function $b(T)$, which correspond to limited polar regions with low temperatures ($T < -20^{\circ}$C), may describe the behaviour of the global function $b(T)$ at low global mean surface temperatures. Thus, it may well be the case that the behaviour of the global function $b_{\mathrm{emp}}(T)$ at low temperatures (dashed line in Fig. 7) cannot be predicted on the basis of the modern regional functions $b(T)$ for low latitudes, making the palaeoclimatic data the only source of information for the corresponding temperature interval. In Fig. 8 we show the potential function $U_{\mathrm{emp}}(T)$, obtained from Eq. (5.1) using the transmissivity function $\widetilde{b}(T)$, which is constructed by merging $b_{\mathrm{emp}}(T)$ (Eq. 6.3) and $b(T)$ (Eq. 5.11):

$$-\frac{dU_{\mathrm{emp}}(T)}{dT} \equiv \widetilde{b}(T)\sigma_R T^4 - a(T)$$
$$\widetilde{b}(T) = \begin{cases} b(T), & T \le 266\,\mathrm{K} \\ b_{\mathrm{emp}}(T), & 266\,\mathrm{K} \le T \le 302\,\mathrm{K} \\ b(T), & T \ge 302\,\mathrm{K} \end{cases} \tag{6.4}$$

The coalbedo $a(T)$ is given by Eq. (5.12). The integration constant in Eq. (6.4) is chosen so that the position of the left extreme of $U_{\mathrm{emp}}(T)$ (complete glaciation) coincides with that of the physical potential function $U(T)$ (Fig. 5).

As is clear from Fig. 8, the stationary state of the modern climate corresponds to a potential pit surrounded by potential barriers. The minimum of the potential pit corresponds to the stationary stable state **2**. The maxima of the surrounding potential barriers corresponds to unstable stationary states, where the probabilities of transition to states **1** and **2** from the left barrier and to states **2** or **3** from the right barrier are

equal.

7 Conclusions: Possible nature of modern climate stability

Solar energy supports all ordered photochemical and dynamic processes on the Earth's surface, including life. The planet absorbs the maximum possible amount of solar energy when the coalbedo is at its maximum (minimal albedo). The stationary state of the modern climate corresponds to coalbedo close to its maximum value possible under terrestrial conditions, $a \approx 0.7$. In the absence of the greenhouse effect, i.e. at $b = 1$, the global mean surface temperature would be equal to the effective temperature of the outgoing long-wave radiation, i.e. $T = T_e = 255$ K (-18°C), making questionable the possibility of life existence. The observed increase of the global mean surface temperature up to the modern optimal for life values ($T_s = +15^{\circ}$C) is only possible due the non-zero greenhouse effect, which corresponds to $b = 0.6$ (see Eq. 5.2). The greenhouse effect is generated by the necessary atmospheric concentrations of greenhouse substances that constitute fractions of per cent of the total atmospheric mass.

The decrease of b from unity to the optimal for life value of 0.6 might retain the physical stability of the stationary surface temperature if only the greenhouse effect is ensured by greenhouse substances with concentrations independent of or only slowly dependent on temperature, like, e.g. CO_2. This will make b practically constant in the vicinity of the stationary temperature. However, the major absorption band of CO_2 traps only 19% of the Earth's thermal radiation at $T = 288$ K (see Eq. 5.5). Even if CO_2 concentration is infinitely increased, which corresponds to disappearance of the second item in sum (Eq. 5.4), the value of b can only be diminished to 0.81. Thus, to reach the needed $b = 0.6$ it is necessary to involve atmospheric water vapour and cloudiness.

However, in the presence of liquid water on the planet's surface, there appears a physical positive feedback between the amount of water vapour and clouds in the atmospheric column (and, consequently, their optical thicknesses m_{H_2O} and m_0) and

the surface temperature (see Eqs. 5.9 and 5.10). With an account made for the non-radiative fluxes of thermal energy (convection and latent heat), this positive feedback makes the stationary surface temperature $T_s = 288$ K physically unstable.

To ensure stability at the same value of surface temperature some controlling processes should be active in the vicinity of this temperature, which will change the basic physical temperature dependence of optical thickness of water vapour and cloudiness.

Differences in the incoming solar fluxes at different latitudes lead to the fact that the equatorial and polar regions are characterised by higher and lower temperatures as compared to the global average, respectively. Processes of global circulation, that arise due to these temperature differences, work to diminish them. An account of global circulation processes is made in the three-dimensional global circulation climate models. If the Earth's surface were entirely flat and perpendicular to the plane of its orbit, all regions would receive equal amounts of solar radiation and the processes of global circulation ceased to exist. It is unlikely that the modern climate stability is due to global circulation processes, i.e. exclusively due to the planetary geometry and peculiarities of the Earth's landscape.

Global circulation processes are unlikely to be able to change significantly the dependence of the greenhouse effect and transmissivity function $b(T)$ on local values of temperature. As discussed above, these local dependencies may cause exponential runaway greenhouse effect in high latitudes, which will contribute to global instability. Moreover, it is unlikely that the global circulation processes are responsible for the drastic increase of the outgoing radiation with decreasing temperature, which takes place at the left and right parts of the zigzag $F_{out}(T)$ (Fig. 7b) and ensures the possibility of modern stationary surface temperature being stable. Within the observed right part of the zigzag, F_{out} changes by more than 60 W m^{-2} within the temperature interval from 299 K to 302 K. This corresponds to 15% of the global mean flux of thermal radiation at the Earth's surface, F_s. In comparison, the average power of global circulation constitues no more than 2.5% of that value (Kellog and Schneider, 1974; Peixoto and Oort, 1984; Chahine, 1992).

One plausible explanation of the observed climate stability that we envisage is the existence of a biotic control of the greenhouse effect (Gorshkov et al., 2000). Without aiming to prove this statement here and considering it as a hypothesis, we list major arguments in its support.

Modern concentrations of all the major greenhouse substances – water vapour, clouds and CO_2 – are under control of the global biota of Earth, being involved into global biogeochemical cycles. Terrestrial vegetation determines the rate of water evaporation from land through regulation of transpiration – release of water vapour from plant leaves (Shukla and Mintz, 1982). In the ocean, the processes of gas exchange are highly dependent upon the abundance of surface-active substances produced by the marine biota (Zutic et al., 1981; Goldman et al., 1988; Frew et al., 1990). Microfilms formed at the sea surface by such substances significantly dampen gas exchange (see, e.g. Asher, 1996), which may impact the values of relative humidity over oceanic surfaces, thus leading to a biotic control of coefficient ε (Eq. 5.10). Regulating concentrations of biotically produced aerosol particles, that constitute a noticeable part of atmospheric aerosols both on land and above the ocean (Pruppacher and Klett, 1978), the biota is able to control ratio r (Eq. 5.9) between optical thicknesses of water vapour and liquid water.

In the ocean, the dominant parameter controlling absorption of the incident solar radiation is the concentration of photosynthetic pigment contained in phytoplankton cells (Sathyendranath, 1991). Regulating this parameter, the marine biota is able to change the average depth at which the short-wave radiation is absorbed and dissipated into heat. The resulting heat flux will thus transfer from different depths, covering different numbers of layers of liquid water m_w (cf. Fig. 1). In the atmosphere, the optical thickness of water vapour is exponentially dependent on temperature (see Eq. 5.10). In contrast, m_w is temperature-independent, being uniquely determined by the average depth where solar radiation is absorbed, which, in its turn, depends on the concentrations of biotically controlled substances. As far as in the stationary case thermal radiation into space is fixed by the value of coalbedo (see Eq. 5.2), it is possible, by

increasing penetration of sunlight into depth, to move a considerable or even dominant part of the greenhouse effect into the ocean. Temperature of the oceanic surface corresponding to $m_w = 0$ will then decrease, an effect similar to the decrease of temperature of the upper atmospheric layers corresponding to small values of optical depth τ. It is not unlikely that the known higher transparency of oligotrophic equatorial waters with respect to solar radiation (Jerlov, 1976) is a manifestation of such biotic cooling of the areas with the largest incoming solar fluxes. On the contrary, in the colder regions the biota may increase turbidity of surface waters, thus making sunlight be absorbed near the surface and generating the full possible greenhouse effect in the atmosphere due to the increase of surface temperature up to the maximum value that is locally possible. Accordingly, the colder regions of the world ocean are known for higher surface concentrations of biological nutrients.

The atmospheric concentration of CO_2, the second important greenhouse gas, is also under biotic control. Given the large number of publications on this topic, here we only note the following. The global biological production (and, consequently, decomposition) is of the order of 10^2 Gt C year^{-1}. The global atmospheric CO_2 content is of the order of 10^3 Gt and coincides in its order of magnitude with the carbon content in the global biota (see, e.g. Sundquist, 1993). Even a minor imbalance in the fluxes of biological production and decomposition may lead to drastic changes of atmospheric CO_2 content over geologically instantaneous time periods, e.g. if biological decomposition exceeds biological production by only 10%, the CO_2 concentration will double in less than 100 years. No geophysical processes are comparable in power with the biological control of atmospheric CO_2.

We note finally that the biological processes (photosynthetic production and metabolic consumption of organic matter) are based on consumption of solar energy. Accordingly, the maximum (Carnot) efficiency η_B of these processes is equal to $\eta_B = (T_{Sun} - T_{Earth})/T_{Sun} \approx (6000\,K - 300\,K)/6000\,K \approx 0.95$ (Gorshkov et al., 2000). In the meantime, the maximum efficiency η_{GC} of the processes of global circulation, which is based on the difference between the temperatures of the polar and equatorial regions, is equal

to $\eta_{GC} = (T_{equator} - T_{poles})/T_{Earth} \approx 30\,K/300\,K \approx 0.1$, which is an order of magnitude lower than η_B. Thus, also from this point of view, the biotic potential for climate control is larger than that of physical dynamic processes on the Earth's surface.

In the modern conditions of increasing anthropogenic impact on the global environment, including human-induced degradation of the natural biota, further investigations into the nature of climate stability on Earth are undoubtedly needed.

Acknowledgements. Work of A. Makarieva is supported by grant No. 00-1596610 of the Russian Foundation for Fundamental Research.

References

Allen, C. W.: Astrophysical Quantities, Athione Press, London, 1955.

Asher, W. E.: The sea-surface microlayer and its effects on global air-sea gas transfer, in: The Sea Surface and Global Change, (Eds) Liss, P. S. and Duce, R. A., Cambridge Univ. Press, New York, pp. 251–285, 1996.

Berggren, W. A. and Van Couvering, J. A. (Eds): Catastrophes and Earth History: The New Uniformitarianism, Princeton Univ. Press, New York, 1984.

Budyko, M. I.: The effect of solar radiation variations on the climate of the earth, Tellus, 21, 611–619, 1969.

Chahine, M. T.: The hydrological cycle and its influence on climate, Nature, 359, 373–380, 1992.

Chandrasekhar, S.: Radiative transfer, Oxford Univ. Press, Oxford, 1950.

Conrath, B. J., Hanel, R. A., Kunde, V. G., and Prabhakara, C.: The infrared interferometer experiment on Nimbus 3, J. Geophys. Res., 75, 5831–5857, 1970.

Dickinson, R. E.: Climate sensitivity, Adv. Geophys., 28A, 99–129, 1985.

Frew, N. M., Goldman, J. C., Dennett, M. R., and Johnson, A. S.: Impact of phytoplankton-generated surfactants on air-sea gas exchange, J. Geophys. Res., 95, 3337–3352, 1990.

Ghil, M.: Climate stability for a Sellers-type model, J. Atmos. Sci., 33, 3–20, 1976.

Goldman, J. C., Dennett, M. R., and Frew, N. M.: Surfactant effects on air-sea gas exchange under turbulent conditions, Deep-Sea Res., 35, 1953–1970, 1988.

Goody, R. M. and Yung, Y. L.: Atmospheric radiation, theoretical basis, 2nd edn., Oxford Univ. Press, New York, 1989.

Gorshkov, V. G., Gorshkov, V. V., and Makarieva, A. M.: Biotic Regulation of the Environment, Key Issue of Global Change, Springer-Praxis Series in Environmental Sciences, Springer-Verlag, London, 2000.

Hibler W. D., III: Modeling sea-ice dynamics, Adv. Geophys., 28A, 549–579, 1985.

Hopf, E.: Mathematical problems of radiative equilibrium, Cambridge Univ. Press, Cambridge, 1934.

Ingersoll, A. P.: The runaway greenhouse: A history of water on Venus, J. Atmos. Sci., 26, 1191–1198, 1969.

Jerlov, N. G.: Marine optics, Elsevier Oceanography Series, 14, Amsterdam, Elsevier, 1976.

Kellogg, W. W. and Schneider, S. H.: Climate stabilisation, for better of for worse? Science, 186, 1163–1172, 1974.

Manabe, S. and Wetherald, R. T.: Thermal equilibrium of the atmosphere with a given distribution of relative humidity, J. Atmos. Sci., 24, 241–259, 1967.

Michalas, D. and Michalas, B. W.: Foundations of radiation hydrodynamics, Oxford Univ. Press, New York, 1984.

Milne E. A.: Thermodynamics of the stars, Handbuch Astrophys., 3, 65–255, 1930.

Mitchell, J.: The "greenhouse" effect and climate change, Rev. Geophys., 27, 115–139, 1989.

Nakajima, S., Hayashi, Y.-Y., and Abe, Y.: A study on the "runaway greenhouse effect" with a one-dimensional radiative-convective equilibrium model, J. Atmos. Sci., 49, 2256–2266, 1992.

North, G. R., Cahalan, R. F., and Coakley, J. A.: Energy balance climate models, Rev. Geophys. Space Phys., 19, 91–121, 1981.

North, G. R. and Coakley, J. A.: Differences between seasonal and mean annual energy balance model calculations of climate and climate sensitivity, J. Atmos. Sci., 36, 1189–1204, 1979.

Peixoto, J. P. and Oort, A. H.: Physics of climate, Rev. Modern Phys., 56, 365–378, 1984.

Pollack, J. B., Toon, O. B., and Boese, R.: Greenhouse models of Venus' high surface temperature, as constrained by Pioneer Venus measurements, J. Geophys. Res., 85, 8223–8231, 1980.

Pruppacher, H. P. and Klett, J. D.: Microphysics of clouds and precipitation, D, Reidel Publishing Company, Dordrecht, Holland, 1978.

Rasool, S. I. and de Berg, C.: The runaway greenhouse and the accumulation of CO_2 in the Venus atmosphere, Nature, 226, 1037–1039, 1970.
Ramanathan, V. and Coakley J. A.: Climate modeling through radiative-convective models, Rev. Geophys. Space Phys., 16, 465–489, 1978.
Raval, A. and Ramanathan, V.: Observational determination of the greenhouse effect, Nature, 342, 758–761, 1989.
Rennó, N. O., Stone, P. H., and Emanuel, K. A.: Radiative-convective model with an explicit hydrological cycle 2. Sensitivity to large changes in solar forcing, J. Geophys. Res., 99D, 17 001–17 020, 1994.
Rodgers, C. D. and Walshaw, C. D.: The computation of infrared cooling rates in planetary atmospheres, Q. J. Roy. Meteorol. Soc., 92, 67–92, 1966.
Rossow, W. B.: Atmospheric circulation of Venus, Adv. Geophys., 28A, 347–379, 1985.
Sathyendranath, S., Gouveia, A. D., Shetye, S. R., Ravindran, P., and Platt, T.: Biological control of surface temperature in the Arabian Sea, Nature, 349, 54–56, 1991.
Savin, S.: The history of the Earth's surface temperature during the past 160 million years, Ann. Rev. Earth Planet. Sci., 5, 319–355, 1977.
Schneider, S. H.: The greenhouse effect: Science and policy, Science, 243, 771–781, 1989.
Stephens, G. L. and Greenwald, T. J.: The Earth's radiation budget and its relation to atmospheric hydrology 1. Observations of the clear sky greenhouse effect, J. Geophys. Res., 96D, 15 311–15 324, 1991a.
Stephens, G. L. and Greenwald, T. J.: The Earth's radiation budget and its relation to atmospheric hydrology 2. Observation of cloud effects, J. Geophys. Res., 96D, 15 325–15 340, 1991b.
Sundquist, E. T.: The global carbon dioxide budget, Science, 259, 934–941, 1993.
Watts, J. A.: The carbon dioxide question: Data sampler, in: Carbon Dioxide Review, (Ed) Clark, W. C., Clarendon Press, New York, 1982.
Weaver, C. P. and Ramanathan, V.: Deductions from a simple climate model: Factors governing surface temperature and atmospheric thermal structure, J. Geophys. Res., 100D, 11 585–11 591, 1995.
Willson, R. C.: Measurements of solar total irradiance and its variability, Space Science Reviews, 38, 203–242, 1984.
Zutic, V. B., Cosovic, B., Marcenko, E., and Bihari, N.: Surfactant production by marine phytoplankton, Mar. Chem., 10, 505–520, 1981.

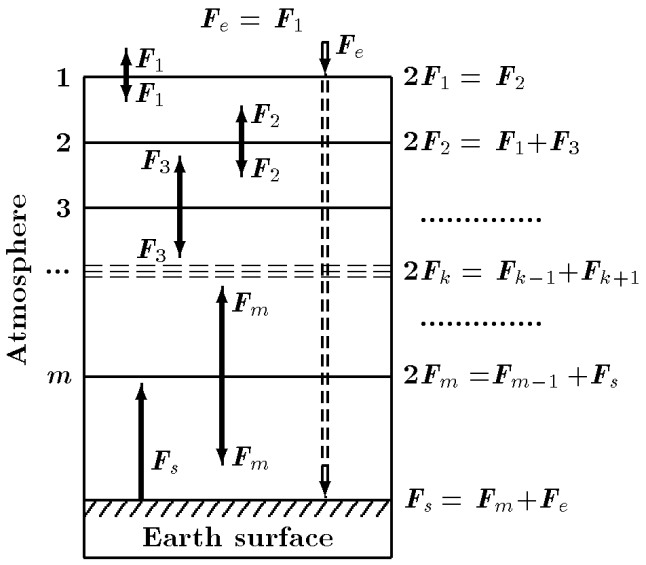

Fig. 1. Dependence of the greenhouse effect on the number m of atmospheric layers absorbing radiation (optical thickness). F_k (k = 1, 2, 3, ..., m) is the flux of radiation emitted by the k-th layer upwards and downwards; F_s is the flux of radiation emitted from the surface; F_e is the outgoing flux of radiation outside the atmosphere equal to the incoming flux of external (solar) radiation absorbed by the surface (empty arrow).

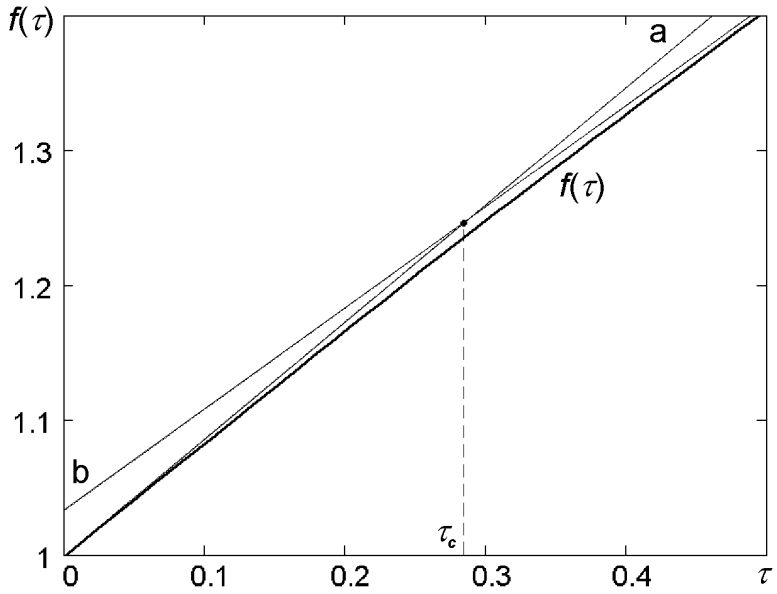

Fig. 2. Dependence of the upwelling thermal radiation flux on optical depth τ. Thick curve: the approximate behaviour of $f(\tau)$, $f(\tau) \equiv F^+(\tau)/F_e = H^+(\tau)/H$, the upwelling thermal radiation flux scaled by the flux of thermal radiation outgoing into space. Thin lines: a = $1 + \frac{\sqrt{3}}{2}\tau$ is the linear assymptote of $f(\tau)$ at $\tau \ll 1$ (see Eq. 3.5); b = $\frac{3}{4}\tau + 1.033$ is the linear assymptote of $f(\tau)$ at $\tau \gg 1$ (see eq. 3.4). Point $\tau_c = 0.28$ marks the area where the switch from the first assymptote to the other approximately takes place.

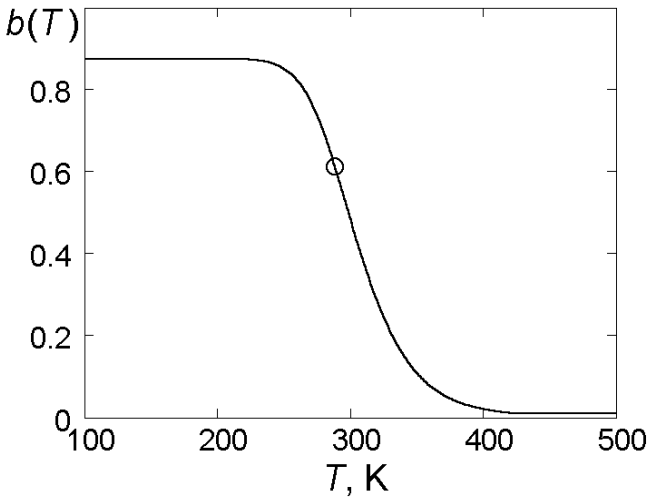

Fig. 3. Temperature dependence (Eq. 5.11) of the theoretical physical transmissivity function $b(T)$. The modern global value $b(288\ \mathrm{K}) = 0.61$ is shown by the empty circle.

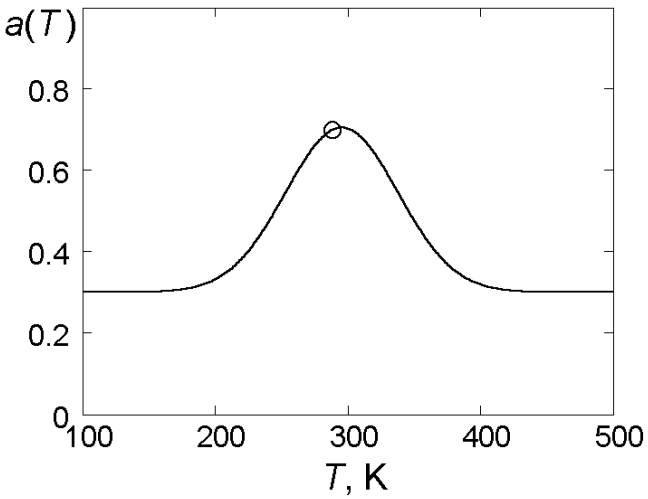

Fig. 4. Temperature dependence (5.12) of the coalbedo $a(T)$. The modern global value a(288 K) = 0.70 is shown by the empty circle.

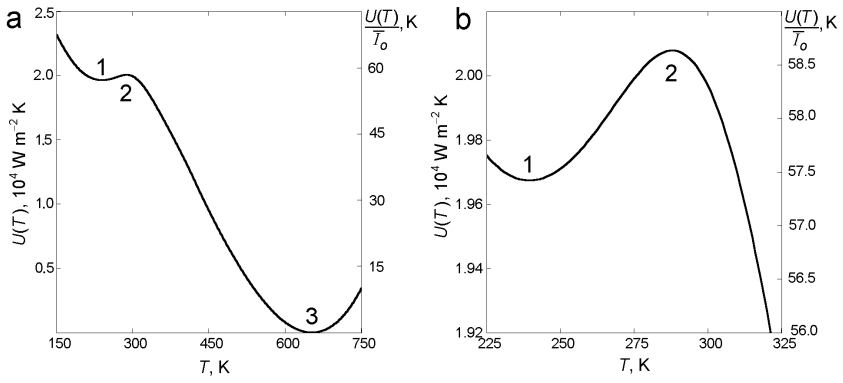

Fig. 5. Theoretical physical potential function $U(T)$ (Eq. 5.1) constructed on the basis of $b(T)$ (Eq. 5.11) and $a(T)$ (Eq. 5.12). States **1** and **3** are stable, corresponding to complete glaciation of the planet and complete evaporation of the hydrosphere, respectively. State **2**, corrsponding to the modern global mean surface temperature, is unstable. **(a)** and **(b)** correspond to different temperature scales.

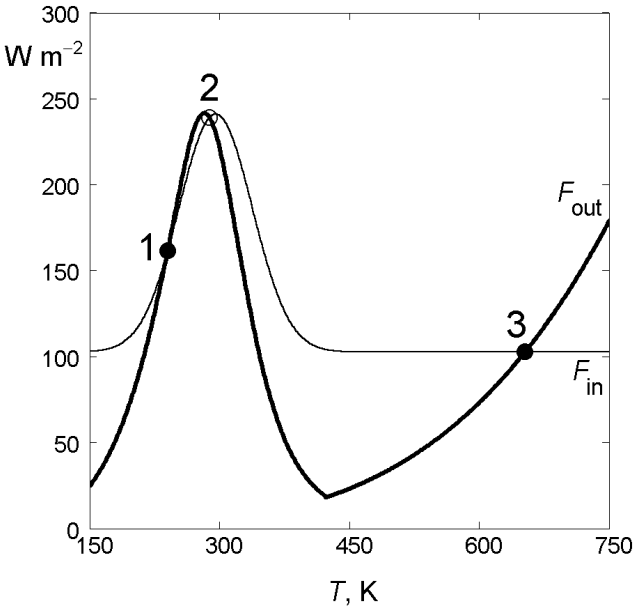

Fig. 6. Theoretical physical dependences of the global mean fluxes $F_{in}(T)$ and $F_{out}(T)$ of the absorbed short-wave (thin line) and emitted by the planet into space long-wave (thick line) radiation on temperature (see Eq. 5.1). The stationary stable points of intersection $F_{in}(T) = F_{out}(T)$ are marked with filled circles. The empty circle shows the unstable stationary state (See legend to Fig. 5 for designations of numbers).

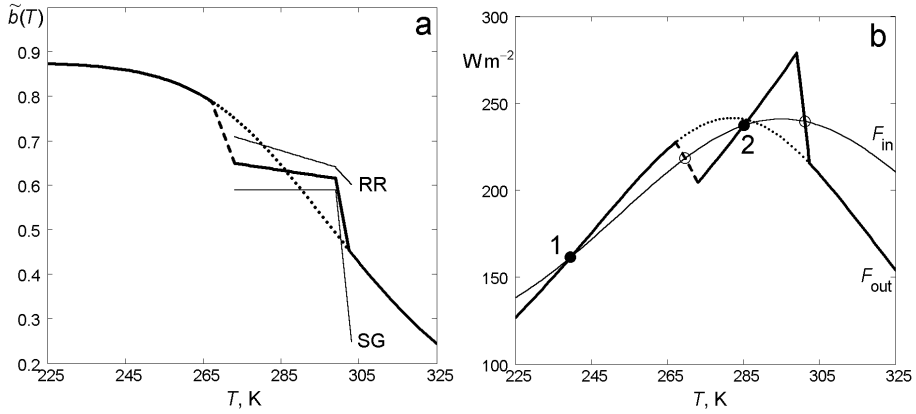

Fig. 7. (a) The observed transmissivity function $b_{emp}(T)$ (Eq. 6.3). RR: function $b_{RR}(T)$ for clear sky (see Eqs. 6.1a and 6.2a). SG: function $b_{SG}(T)$ for cloudy sky (see Eqs. 6.1b and6.2b). Thick solid curve interrupted by dashed line: function $\tilde{b}(T)$ (see Eqs. 6.3 and 6.4). The dashed line corresponds to the tentative temperature interval where the behaviour of $b_{emp}(T)$ remains unknown. Dotted curve: theoretical function $b(T)$ (Eq. 5.11) in the temperature interval 266 K $\leq T \leq$ 302 K (see Fig. 3). **(b)** Temperature dependence of the outgoing flux of long-wave radiation, $F_{out}(T)$, taking into account its observed behaviour in the vicinity of modern global mean surface temperature. Thick curve interrupted by dashed line: $F_{out}(T) \equiv \tilde{b}(T)\sigma_R T^4$. Dotted curve: theoretical physical behaviour of F_{out} (see Fig. 6). Thin curve: the global mean flux of the absorbed solar radiation $F_{in}(T)$ (see Fig. 6). The stationary stable points of intersection $F_{in}(T) = F_{out}(T)$, corresponding to complete glaciation (**1**) and modern climate (**2**) are marked with filled circles. The empty circles show the unstable stationary states corresponding to potential stability barriers of the modern climate (see Fig. 8).

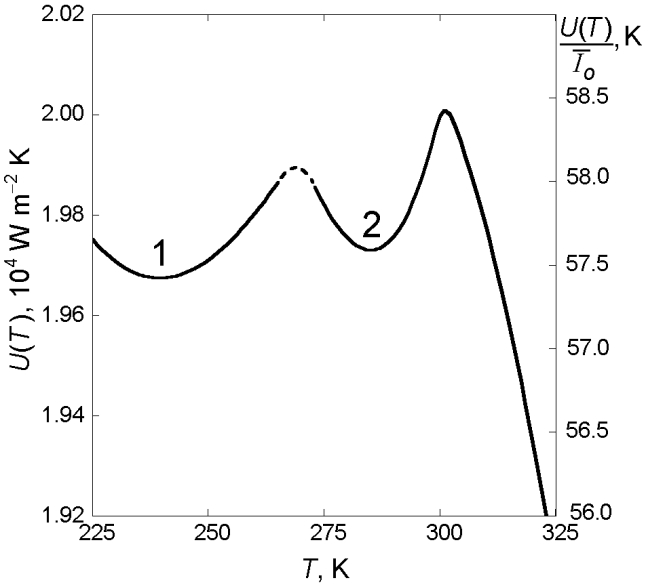

Fig. 8. The potential function $U_{emp}(T)$ (Eq. 6.4) of the modern Earth's climate. Dashed line, as in Figs. 7a, b, corresponds to the region of the unknown behaviour of $b_{emp}(T)$ (Eq. 6.3).